Title

MR imaging pattern of tibial subchondral bone structure: considerations of meniscal coverage and integrity

Journal

Skeletal Radiology, 49(12)

ISSN

0364-2348

Authors

Ariyachaipanich, Aticha
Kaya, Emel
Statum, Sheronda
et al.

Publication Date

2020-12-01

DOI

10.1007/s00256-020-03517-6

Peer reviewed

HHS Public Access

Author manuscript

Skeletal Radiol. Author manuscript; available in PMC 2021 December 01.

Published in final edited form as:

Skeletal Radiol. 2020 December ; 49(12): 2019–2027. doi:10.1007/s00256-020-03517-6.

MR Imaging Pattern of Tibial Subchondral Bone Structure: Considerations of Meniscal Coverage and Integrity

Aticha Ariyachaipanich, MD[2,3,4], **Emel Kaya, MD**[2,5], **Sheronda Statum, MS, MBA**[1,2], **Reni Biswas, BS**[1,2], **Betty Tran, BS**[1,2], **Won C. Bae, PhD**[1,2], **Christine B. Chung, MD**[1,2]

[1]Department of Radiology, VA San Diego Healthcare System, San Diego, CA [2]Department of Radiology, University of California-San Diego, La Jolla, CA [3]Department of Radiology, King Chulalongkorn Memorial Hospital, The Thai Red Cross Society, Bangkok, Thailand [4]Department of Radiology, Faculty of Medicine, Chulalongkorn University, Bangkok, Thailand [5]Radiology Department, Istanbul Bilim University, Istanbul, Turkey

Abstract

Objectives.—To compare regional differences in subchondral trabecular structure using high-resolution MRI in meniscal-covered/ uncovered tibia in cadaveric knees with intact/torn menisci.

Materials and Methods.—3-D proton-density CUBE MRI of 6 cadaveric knees without significant osteoarthritis (OA) was acquired, 0.25-mm resolution. Menisci were evaluated and classified intact or torn. MR data were transferred to ImageJ program to segment tibial 3D volume of interest (VOI). Data was subdivided into meniscus-covered/ uncovered regions. Segmented VOI was classified into binary data, trabeculae/bone marrow. The trabecular bone data was used to measure MR biomarkers (apparent subchondral plate connected bone density (adapted from spine MR), apparent trabecular bone volume fraction, apparent mean trabecular thickness, apparent connectivity density, and structure model index (SMI). Mean value of parameters were analyzed for effects of meniscal tear/tibial coverage.

Results.—9 torn menisci and 3 intact menisci were present. MR measures of bone varied significantly due to meniscal coverage/tear. Subchondral plate connected bone density under covered meniscus regions increased from 10.9% to23.5% with meniscal tear. Values increased in uncovered regions, 19.3% (intact) and 32.4% (torn). This reflects higher density when uncovered ($p=0.048$) with meniscal tear ($p=0.007$). Similar patterns were found for trabecular bone fraction (coverage $p<0.001$, tear $p=0.047$), trabecular thickness (coverage $p=0.03$), connectivity density (coverage $p=0.002$), and SMI (coverage $p=0.015$).

Corresponding Author: Christine B. Chung, MD, [1]Department of Radiology, VA San Diego Healthcare System, cbchung@ucsd.edu.

Declaration of competing interest

The authors declare no conflict of interest.

Conclusion.—Quantitative trabecular bone evaluation emphasizes intrinsic structural differences between meniscal covered/uncorered tibia. Results offer insight into bone adaptation with meniscal tear and support hypothesis that subchondral bone plate connected bone density could be important in early subchondral bone adaptation.

Keywords

Knee; Osteoarthritis; Meniscal Tear; Trabeculae; Morphometry; MRI

Introduction

Meniscal tears are commonly encountered pathology in osteoarthritic patients, found in about 67% of asymptomatic and 91% of symptomatic patients [1]. It is also reported in 0.7 per 1000 patients-year in acute knee injury treated at emergency departments [2]. The patients who have meniscal tear or meniscectomy are at increased risk of developing osteoarthritis [3-5]. Further, osteoarthritic patients with concomitant meniscal tear have been shown to present with more rapid cartilage loss [6, 7]. These findings support the critical role of the meniscus for preservation of knee structure, normal knee function, and biomechanics.

The primary functions of meniscus include load distribution and shock absorption [8-12]. This is emphasized by the disparate nature of the articular structures beneath the meniscus-covered versus meniscus-uncovered regions of the tibia [13-16]. The density of the subchondral bone and thickness of cartilage beneath the meniscus-covered region has been reported to be less than its covered counterpart [14]. In the setting of partial and total meniscectomy, increased focal stress on the bone is evidenced through increased bone density [14, 17, 18]. Trabecular bone structure is dynamic and has the potential to adapt to its loading environment [19]. Clearly, the structure and function of the meniscus and underlying articular surface are related through the concept of the meniscal-osteochondral unit. In addition, there is a body of literature that suggests a biologic link between the subchondral bone and articular cartilage, whereby the former initiates or drives progression of OA [20-22].

Currently, many magnetic resonance imaging (MRI) biomarkers that characterize trabecular bone have been introduced in the literature. To date, most studies focusing on trabecular assessment have addressed osteoporosis and osteoarthritis, emphasizing global osseous remodeling. In the setting of knee osteoarthritis, results have highlighted the importance of interactions of trabecular bone, cartilage and meniscus in its pathogenesis as well as the development of tools to assess these interactions in the clinical setting. Interest from the academic and clinical community stems from the noninvasive nature of MR imaging, improved workflow through obviating the need for additional testing to characterize bone, and the lack of ionizing radiation associated with CT assessment.

We implemented the conventional MR parameters for trabecular bone assessment in subregions of the tibia with meniscal pathology in the absence of OA, and adapted an additional biomarker previously implemented in lumbar vertebral body trabecular evaluation [23]. This parameter assesses the vertical trabeculae that connect to the subchondral bone

plate, and in the spine were established as important primary contributors to bone strength. We hypothesize that changes in load distribution after meniscal tear will result in regional trabecular adaptation. To the best of our knowledge, this is the first MR study to correlate the regional subchondral trabecular characteristics in a whole joint cadaveric model with regard to meniscal coverage and overlying regional meniscal integrity without underlying OA, as well as the first evaluation of the relationship of vertical trabecular bone with subchondral bone connectivity in the knee.

Materials and Methods

Subjects

A total of 6 knees were scanned from 3 cadaveric donors (2 females and 1 male) with mean age 78.6 years old (64, 79 and 93 years of age at death) without underlying OA. No history of osteoporosis, renal failure, osteomalacia, bisphosphonate or steroid use was noted in the medical history available. This study was approved by the institutional review board.

Image acquisition

A 3-Tesla MR scanner (Discovery 750, General Electric healthcare systems, Waukesha, WI) and a dedicated 8 channel knee coil (InVivo Corporation, Gainesville, FL, USA) were used for image acquisition. High-resolution MR images (Figure 1) were acquired for assessing the trabecular bone structure and meniscal pathology using a 3-dimensional (3D) CUBE fast spin echo sequence (chosen to minimize susceptibility artifact in trabecular bone apparent in 3D gradient echo sequences). MR images were obtained in the sagittal plane with the following parameters: time-to-repeat (TR) = 1500 ms, time-to-echo (TE) = 30 ms, flip angle = 90°, matrix = 320x320, slice thickness = 0.4 mm, number of slices = 450 to 510, field of view (FOV) = 13 cm, echo train length (ETL) = 25, bandwidth = ±31.25 kHz, no fat suppression, with an approximate scan time of 10 minutes. The image resolution was 0.4 mm isotropic, interpolated to 0.25 mm using ImageJ in post-processing.

Two musculoskeletal radiologists evaluated MR findings individually. Meniscal pathology was classified as intact, or tear in the anterior horn, mid-body, and posterior horn. Commonly accepted imaging criteria for tear diagnosis was implemented [24]. In the case of disagreement, the findings were reevaluated by consensus. None of the cadaveric specimens met criteria for significant OA based upon classic MR scoring systems in early or advanced OA [25]. No osteophyte formation, high-grade chondral loss or altered marrow signal was noted in regions of meniscal tear or elsewhere in the joint. In the setting of OA, full thickness chondral loss in a region of 10 mm^2 is considered significant. Neither this, nor areas of greater than 50% chondral thickness loss were identified in the specimens.

MR data were transferred to the ImageJ program [26] to segment 3D volumes of interest (VOI) representing the trabecular bone and marrow of the proximal tibia. The tibial trabecular bone was then subdivided into 4 regions (Figure 1): 1) directly covered by the medial meniscus, 2) directly covered by the lateral meniscus, 3) medial tibial meniscus-uncovered, and 4) lateral tibial meniscus-uncovered regions. To achieve this, menisci, excluding meniscal root and ligament, were manually segmented on sequential sagittal

images (Figure 1). The meniscus-uncovered region was designated by the area enclosed by the inner border of the meniscal tissue and a line drawn from anterior horn to posterior horn (Figure 1A, green dotted line). Using BoneJ plug-in [27], we determined standard trabecular bone morphometric measures [28] of 10-mm thick volume beneath the subchondral bone plate (ScP). These included apparent bone volume fraction (app BVF), apparent mean trabecular thickness (app Tb,Th), apparent connectivity density (app CD) and structure model index (SMI). SMI is an index to determine the plate- or rod-like trabecular structure where the theoretical value for a perfect rod-like trabeculae is 3 and perfect plate-like trabeculae is 0 [27, 28]. A lower SMI value reflects a higher ratio of the plate-like to rod-like structures.

A custom Matlab program (R2011b, MathWorks, Natick, MA) was written for analysis of trabeculae connected to subchondral bone plate (ScP) and to visualize local changes. Global tibial VOI (i.e., manual segmentation of tibial trabecular bone, whose superior surface represents the bottom of the ScP) was applied to 3D CUBE MR data in order to determine the bottom of the ScP (Figure 2A, top blue line), and then offset 0.25 mm (Figure 2A, middle red line) to segment a thin slab of trabecular bone “connected” to the ScP. The surface was also offset 10 mm (Figure 2A, bottom orange line) to segment 10 mm-thick slab of trabecular bone for creating color map of trabecular bone volume fraction. The 10 mm thickness was based upon established analysis of tibial trabecular strength [29]. The segmented data were thresholded (Figure 2A, black and white insert) by connectivity optimization [27] to create binary data. For visualization purposes, axially flattened mean intensity projection images of ScP “connected” trabecular bone (Figure 2B and Figure 3AB) and of 10-mm thick slab of trabecular bone (Figure 2C) were created. Trabecular parameters obtained from MRI are likely over-estimated compared to the actual values (from histomorphometry or micro computed tomography) due to limited spatial resolution. Therefore, all MR parameters were considered as “apparent” structural parameters. The binary data of the 0.25-mm thin slab was used to determine the volume of ScP-connected trabeculae divided by the total volume to determine apparent ScP connected bone density (Figure 5). Binary data of 10-mm thick slab was used to create axial mean intensity projection images (Figure 2C and Figure 4AB) as well as axial color map of bone volume fraction (Figure 4CD). The color maps were created using a moving window filter applied over the entire tibial plateau, providing a way to observe localized changes in bone volume fraction. A pseudo code is provided in Appendix 1.

For statistical analysis, quantitative bone measures were averaged at the four VOI defined by meniscus-covered and –uncovered regions, and analyzed for the effects of meniscal coverage (repeated factor) and tear (intact vs. torn) on the mean values using two-way repeated measures analysis of variance (ANOVA) performed with a commercial software (Systat 10, Systat Software Inc., San Jose, CA). Significance level was set at $p=0.05$ (two-tailed, as the measured values could either increase or decrease), and post hoc power for each factor was determined using G*Power software. In general the analysis was underpowered due to the small number of samples, and the study may have been biased due the treatment of bilateral knees as independent samples.

Results

Meniscal pathology in the 6 cadaveric knees are shown in Table 1. There were 3 intact and 9 torn menisci. No meniscal tears appeared macerated or had displaced meniscal flaps/ fragments. Four of the nine appeared complex (more than one linear area of signal extending to an articular surface). The measured MR parameters, p-values, and power values are listed in Table 2. Figure 5 and 6 are plots of the mean and the standard error values.

Meniscal coverage demonstrated statistically significant effect in all MR parameters. Meniscus-uncovered regions had greater apparent ScP connected bone density (Figure 5), app BVF (Figure 6A), app Tb.Th (Figure 6B), app CD (Figure 6C) and lower SMI values (Figure 6D) compared to meniscus-covered regions in all samples irrespective of meniscal tear. However, as shown in Table 2, the statistical power was generally low and highly variable due to the small number of samples.

Additionally, apparent ScP connected bone density (Figure 5) and app BVF (Figure 6A) were significantly higher in regions under the torn menisci compared to those under intact menisci. The rest of MR parameters demonstrated no significant differences between torn and intact menisci. Subsequent analysis of the statistical interaction between meniscal integrity (intact vs. torn) and coverage (meniscus-covered vs. -uncovered regions) was not statistically significant for any MR parameters.

Color maps of app BVF (Figures 4CD) were visually consistent with the quantitative findings above. Overall higher values of app BVF were observed in meniscus-uncovered regions as well as under the torn menisci. While it appears that location of the meniscal tear (Figure 7, white arrows) may be related to focal changes in bone measures underneath (Figure 7, orange arrows), this remains to be evaluated further.

Discussion

To the best of our knowledge, the present study is the first to provide regional quantitative MR assessment of subchondral trabecular bone, emphasizing the meniscal covered and uncovered tibial articular surface without underlying osseous or chondral degeneration. The study further explored the relationship of meniscal tear and MR bone biomarkers in this regional analysis. The importance of the osteochondral junction and the concept of the meniscal osteochondral unit have been stressed in the literature [30, 31]. The traditional view of OA as a disease of articular cartilage has been challenged with more complex theories that note interplay between subchondral bone and cartilage [22]. The potential role of abnormal subchondral trabecular bone metabolism in the initiation and/or progression of OA, a sort of inside-out theory of OA occurring independent of and preceding cartilage degeneration, has been discussed in the literature [20, 21]. To fully leverage the data acquired from MR bone biomarkers for the purpose of exploring the pathogenesis of OA, patterns of bone structure encountered in tissue without OA must be established. Only then can we begin to interrogate bone interactions with meniscus and other tissue failure.

The meniscus normally functions to facilitate load distribution and shock absorption. In so doing, it shields the underlying osteochondral tissues from the direct joint contact forces,

which may explain the differences between the structures of the meniscal-covered vs. – uncovered cartilage and bone. Our quantitative MR results in samples with intact menisci are similar to past studies that utilized histologic reference measurements [14, 15]. Axial color map of app BVF (Figure 4C) showed spatial distribution congruous with the quantitative findings: in samples with intact menisci, the color maps showed high values in medial meniscus-uncovered region and posterior half of lateral tibia plateau. This was also consistent with maps of joint contact regions and force distribution determined in the tibial plateau [9]. In addition, apparent ScP connected bone density, a newly introduced osteochondral junction biomarker, also demonstrated a higher value in the uncovered region. Evaluation of spine trabecular samples showed that bone volume fraction of vertical trabeculae better predicted mechanical behavior than did bone volume fraction of the entire specimen [32]. The importance of vertical trabeculae, and connectivity to subchondral bone is further supported by biomechanical data noting primary tibial bone strength predominates within 5 mm of the subchondral bone plate. The data acquired in this study is limited and requires further interrogation.

Alterations in tibial bone structure in the samples with torn menisci suggest adaptation to changes in the mechanical environment of the knee. The meniscus dissipates load by a reported 45-60% [33]. In case of meniscectomy or meniscal tear, the disruption in hoop strength can result in increased compressive load by 40-700% [8, 9, 34]. The change in cortical and trabecular bone occurs as an adaptation to load alteration, such as during immobilization [35] or induced joint instability [36, 37] in animals. After meniscectomy, studies have generally found overall increases in ScP thickness and trabecular BVF [37, 38], although a few have found decreased BVF in the setting of meniscal pathology [38]. Our results of increased ScP connected bone density, app BVF, and app Tb.Th., in samples with torn menisci are consistent with the past findings. Of note, the changes in bone biomarkers in the setting of meniscal tear are occurring without underlying OA, and with preservation of articular cartilage. The suggestion that location of meniscal tear may correlate with focal trabecular remodeling (Figure 7) provides an avenue for further exploration in the setting of isolated meniscal pathology.

A major technical limitation of this MR study is low image resolution. Trabecular thickness in the proximal tibia is about 0.1 to 0.2 mm. The resolution in this study was 0.4 mm. It has been demonstrated that the trabecular bone parameters become overestimated as the voxel size increases, and this is most pronounced for the trabecular thickness [39]. Nonetheless, there is a strong ($R>0.8$) correlation between the bone measures calculated using large voxel (264 um) vs. and the reference small voxel (65 um) images in the past studies [39]. Although the spatial resolution in our study was limited, it is similarly sufficient to detect relative differences between samples. Another limitation is the cross-sectional study design with a small number of samples. The study does, however, serve as a pilot for larger scale evaluation emphasizing feasibility in an OA cohort. Additionally, while we have not validated the imaging and analysis techniques against a reference standard in this study, MR measures of bone structure have been shown to correlate with bone mineral density from dual-energy X-ray absorptiometry [40] and quantitative computed tomography [41, 42], with a good reproducibility [40, 43-45]. Sensitivity of MR bone measures to aging and disease has also been previously demonstrated [46, 47].

A consideration for future work is the biomechanical differences between medial and lateral compartments, taking into consideration trabecular structural patterns. It has been reported that the lateral meniscus is more mobile than the medial meniscus [48] while the strength and load distribution is greater on the medial compartment [8, 9, 29, 34]. Additionally, not all meniscal tears had equal effect on meniscal mechanical axis alteration [49]. In light of these, a subgroup analysis with consideration to medial versus lateral menisci, as well as inclusion of various types of tears will offer great insight into bone adaptation characterization in the future. Unfortunately, due to small number of samples and different proportion of torn menisci on lateral vs. medial sides, we could not show their relative involvement at this time. Lastly, it would have been useful to have a negative control for the trabecular measures, for example samples taken from tibial diaphysis or distal femur, to demonstrate no inherent difference between right vs. left lower extremities within an individual. These additional testing remain to be performed to further validate the utility of our techniques.

In conclusion, we provide the first quantitative MR verification of regional differences in bone biomarkers between the meniscal covered and uncovered regions of the tibial plateau. The identification of this pattern is crucial for interrogation of the role of subchondral bone in initiation and progression of OA. Our results of increased ScP connected bone density and app BVF, in samples with torn menisci are consistent with the past findings. Of note, the changes in bone biomarkers in the setting of meniscal tear are occurring without underlying OA, and with preservation of articular cartilage.

Conclusion

Results from quantitative trabecular bone evaluation emphasize the intrinsic structural differences between the meniscal covered and uncovered tibial articular surface. Further, results offer insight into bone adaptation in the setting of meniscal tear without significant OA and support the hypothesis that apparent subchondral bone plate connected bone density could be an important consideration in early subchondral bone adaptation mechanisms.

Acknowledgments

Research reported in this publication was supported by grants from the Clinical Science Research & Development of the Veterans Affairs Office of Research and Development (Award Number 5I01CX000625; Project ID: 1161961) in support of Dr. Christine B. Chung, and the National Institute of Arthritis and Musculoskeletal and Skin Diseases (NIAMS) of the National Institute of Health (NIH) in support of Dr. Christine Chung (Award Number R01 AR064321) and Dr. Won C. Bae (Award Number R01 AR066622). The contents of this paper are solely the responsibility of the authors and do not necessarily represent the official views of the funding agencies.

References

1. Bhattacharyya T, Gale D, Dewire P, Totterman S, Gale ME, McLaughlin S, et al. The clinical importance of meniscal tears demonstrated by magnetic resonance imaging in osteoarthritis of the knee. The Journal of bone and joint surgery American volume. 2003; 85-A:4–9.
2. Nielsen AB, Yde J. Epidemiology of acute knee injuries: a prospective hospital investigation. The Journal of trauma. 1991; 31:1644–1648. [PubMed: 1749037]
3. Badlani JT, Borrero C, Golla S, Harner CD, Irrgang JJ. The effects of meniscus injury on the development of knee osteoarthritis: data from the osteoarthritis initiative. The American journal of sports medicine. 2013; 41(6):1238–1244. [PubMed: 23733830]

4. Cicuttini FM, Forbes A, Yuanyuan W, Rush G, Stuckey SL. Rate of knee cartilage loss after partial meniscectomy. The Journal of rheumatology. 2002; 29:1954–1956. [PubMed: 12233892]
5. Roos H, Lauren Mr, Adalberth T, Roos EM, Jonsson K, Lohmander LS. Knee osteoarthritis after meniscectomy: Prevalence of radiographic changes after twenty-one years, compared with matched controls. Arthritis and rheumatism. 1998; 41:687–693. [PubMed: 9550478]
6. Biswal S, Hastie T, Andriacchi TP, Bergman GA, Dillingham MF, Lang P. Risk factors for progressive cartilage loss in the knee: a longitudinal magnetic resonance imaging study in forty-three patients. Arthritis and rheumatism. 2002; 46:2884–2892. [PubMed: 12428228]
7. Hunter DJ, Zhang YQ, Niu JB, Tu X, Amin S, Clancy M, et al. The association of meniscal pathologic changes with cartilage loss in symptomatic knee osteoarthritis. Arthritis and rheumatism. 2006; 54(3):795–801. [PubMed: 16508930]
8. Kurosawa H, Fukubayashi T, Nakajima H. Load-bearing mode of the knee joint: physical behavior of the knee joint with or without menisci. Clinical orthopaedics and related research. 1980(149):283–290.
9. Fukubayashi T, Kurosawa H. The contact area and pressure distribution pattern of the knee. A study of normal and osteoarthrotic knee joints. Acta orthopaedica Scandinavica. 1980; 51(6):871–879. [PubMed: 6894212]
10. Ahmed AM, Burke DL. In-vitro measurement of static pressure distribution in synovial joints--Part I: Tibial surface of the knee. J Biomech Eng. 1983; 105(3):216–225. [PubMed: 6688842]
11. Paletta GA Jr., Manning T, Snell E, Parker R, Bergfeld J. The effect of allograft meniscal replacement on intraarticular contact area and pressures in the human knee. A biomechanical study. The American journal of sports medicine. 1997; 25(5):692–698. [PubMed: 9302479]
12. Walker PS, Arno S, Bell C, Salvadore G, Borukhov I, Oh C. Function of the medial meniscus in force transmission and stability. Journal of biomechanics. 2015; 48:1383–1388. [PubMed: 25888013]
13. Iijima H, Aoyama T, Ito A, Tajino J, Nagai M, Zhang X, et al. Immature articular cartilage and subchondral bone covered by menisci are potentially susceptive to mechanical load. BMC musculoskeletal disorders. 2014; 15:101. [PubMed: 24669849]
14. Noble J, Alexander K. Studies of tibial subchondral bone density and its significance. The Journal of bone and joint surgery American volume 1985:295–302. [PubMed: 3881450]
15. Thambyah A, Nather A, Goh J. Mechanical properties of articular cartilage covered by the meniscus. Osteoarthritis and cartilage / OARS, Osteoarthritis Research Society. 2006; 14(6):580–588.
16. Milz S, Putz R. Quantitative morphology of the subchondral plate of the tibial plateau. Journal of anatomy. 1994; 185:103–110. [PubMed: 7559105]
17. Lee SJ, Aadalen KJ, Malaviya P, Lorenz EP, Hayden JK, Farr J, et al. Tibiofemoral contact mechanics after serial medial meniscectomies in the human cadaveric knee. The American journal of sports medicine. 2006; 34(8):1334–1344. [PubMed: 16636354]
18. McKinley TO, English DK, Bay BK. Trabecular bone strain changes resulting from partial and complete meniscectomy. Clinical orthopaedics and related research 2003:259–267.
19. Wolff J The classic: on the inner architecture of bones and its importance for bone growth. 1870. Clinical orthopaedics and related research. 2010; 468(4):1056–1065. [PubMed: 20162387]
20. Lajeunesse D, Reboul P. Subchondral bone in osteoarthritis: a biologic link with articular cartilage leading to abnormal remodeling. Curr Opin Rheumatol. 2003; 15(5):628–633. [PubMed: 12960492]
21. Tu M, Yang M, Yu N, Zhen G, Wan M, Liu W, et al. Inhibition of cyclooxygenase-2 activity in subchondral bone modifies a subtype of osteoarthritis. Bone Res. 2019; 7:29. [PubMed: 31666999]
22. Xie L, Tintani F, Wang X, Li F, Zhen G, Qiu T, et al. Systemic neutralization of TGF-beta attenuates osteoarthritis. Annals of the New York Academy of Sciences. 2016; 1376(1):53–64. [PubMed: 26837060]
23. Fields AJ, Lee GL, Liu XS, Jekir MG, Guo XE, Keaveny TM. Influence of vertical trabeculae on the compressive strength of the human vertebra. Journal of bone and mineral research : the official journal of the American Society for Bone and Mineral Research. 2011; 26(2):263–269.

24. Subhas N, Sakamoto FA, Mariscalco MW, Polster JM, Obuchowski NA, Jones MH. Accuracy of MRI in the diagnosis of meniscal tears in older patients. AJR American journal of roentgenology. 2012; 198(6):W575–580. [PubMed: 22623573]
25. Hunter DJ, Arden N, Conaghan PG, Eckstein F, Gold G, Grainger A, et al. Definition of osteoarthritis on MRI: results of a Delphi exercise. Osteoarthritis and cartilage / OARS, Osteoarthritis Research Society. 2011; 19(8):963–969.
26. Schindelin J, Arganda-Carreras I, Frise E, Kaynig V, Longair M, Pietzsch T, et al. Fiji: an open-source platform for biological-image analysis. Nature methods. 2012; 9(7):676–682. [PubMed: 22743772]
27. Doube M, Klosowski MM, Arganda-Carreras I, Cordelieres FP, Dougherty RP, Jackson JS, et al. BoneJ: Free and extensible bone image analysis in ImageJ. Bone. 2010; 47(6):1076–1079. [PubMed: 20817052]
28. Zhang Y, He Z, Fan S, He K, Li C. Automatic Thresholding of Micro-CT Trabecular Bone Images. 2008:23–27.
29. Harada Y, Wevers HW, Cooke TD. Distribution of bone strength in the proximal tibia. The Journal of arthroplasty. 1988; 3(2):167–175. [PubMed: 3397747]
30. Chang EY, Chen KC, Chung CB. The shiny corner of the knee: a sign of meniscal osteochondral unit dysfunction. Skeletal radiology. 2014; 43(10):1403–1409. [PubMed: 25052537]
31. Kumar D, Schooler J, Zuo J, McCulloch CE, Nardo L, Link TM, et al. Trabecular Bone Structure and Spatial Differences in Articular Cartilage MR Relaxation Times in Individuals with Posterior Horn Medial Meniscal Tears. Osteoarthritis and cartilage / OARS, Osteoarthritis Research Society. 2013; 21:86–93.
32. Liu XS, Sajda P, Saha PK, Wehrli FW, Bevill G, Keaveny TM, et al. Complete volumetric decomposition of individual trabecular plates and rods and its morphological correlations with anisotropic elastic moduli in human trabecular bone. Journal of bone and mineral research : the official journal of the American Society for Bone and Mineral Research. 2008; 23(2):223–235.
33. Seedhom BB, Dowson D, Wright V. Proceedings: Functions of the menisci. A preliminary study. Annals of the rheumatic diseases. 1974; 33(1):111. [PubMed: 4821376]
34. Baratz ME, Fu FH, Mengato R. Meniscal tears: the effect of meniscectomy and of repair on intraarticular contact areas and stress in the human knee. A preliminary report. The American journal of sports medicine. 1986; 14(4):270–275. [PubMed: 3755296]
35. Jozsa L, Reffy A, Jarvinen M, Kannus P, Lehto M, Kvist M. Cortical and trabecular osteopenia after immobilization. A quantitative histological study of the rat knee. International orthopaedics. 1988; 12(2):169–172. [PubMed: 3045030]
36. Botter SM, Glasson SS, Hopkins B, Clockaerts S, Weinans H, van Leeuwen JP, et al. ADAMTS5−/− mice have less subchondral bone changes after induction of osteoarthritis through surgical instability: implications for a link between cartilage and subchondral bone changes. Osteoarthritis and cartilage / OARS, Osteoarthritis Research Society. 2009; 17(5):636–645.
37. Fahlgren A, Messner K, Aspenberg P. Meniscectomy leads to an early increase in subchondral bone plate thickness in the rabbit knee. Acta orthopaedica Scandinavica. 2003; 74(4):437–441. [PubMed: 14521295]
38. Petersen MM, Olsen C, Lauritzen JB, Lund B, Hede A. Late changes in bone mineral density of the proximal tibia following total or partial medial meniscectomy. A randomized study. Journal of orthopaedic research : official publication of the Orthopaedic Research Society. 1996; 14(1):16–21. [PubMed: 8618160]
39. Kim N, Lee J-G, Song Y, Kim HJ, S Yeom J, Cho G. Evaluation of MRI resolution affecting trabecular bone parameters: determination of acceptable resolution. Magnetic resonance in medicine. 2012; 67:218–225. [PubMed: 21656550]
40. Krug R, Banerjee S, Han ET, Newitt DC, Link TM, Majumdar S. Feasibility of in vivo structural analysis of high-resolution magnetic resonance images of the proximal femur. Osteoporosis international : a journal established as result of cooperation between the European Foundation for Osteoporosis and the National Osteoporosis Foundation of the USA. 2005; 16:1307–1314.

41. Hong J, Hipp JA, Mulkern RV, Jaramillo D, Snyder BD. Magnetic resonance imaging measurements of bone density and cross-sectional geometry. Calcified tissue international. 2000; 66:74–78. [PubMed: 10602850]

42. Krug R, Carballido-Gamio J, Burghardt AJ, Kazakia G, Hyun BH, Jobke B, et al. Assessment of trabecular bone structure comparing magnetic resonance imaging at 3 Tesla with high-resolution peripheral quantitative computed tomography ex vivo and in vivo. Osteoporosis International. 2008; 19:653–661. [PubMed: 17992467]

43. Gomberg BR, Wehrli FW, Vasilic B, Weening RH, Saha PK, Song HK, et al. Reproducibility and error sources of micro-MRI-based trabecular bone structural parameters of the distal radius and tibia. Bone. 2004; 35(1):266–276. [PubMed: 15207767]

44. Alberich-Bayarri A, Marti-Bonmati L, Sanz-Requena R, Sanchez-Gonzalez J, Hervas Briz V, Garcia-Marti G, et al. [Reproducibility and accuracy in the morphometric and mechanical quantification of trabecular bone from 3 Tesla magnetic resonance images]. Radiologia. 2014; 56(1):27–34. [PubMed: 24094441]

45. Beuf O, Ghosh S, Newitt DC, Link TM, Steinbach L, Ries M, et al. Magnetic resonance imaging of normal and osteoarthritic trabecular bone structure in the human knee. Arthritis and rheumatism. 2002; 46(2):385–393. [PubMed: 11840441]

46. Majumdar S, Kothari M, Augat P, Newitt DC, Link TM, Lin JC, et al. High-resolution magnetic resonance imaging: three-dimensional trabecular bone architecture and biomechanical properties. Bone. 1998; 22:445–454. [PubMed: 9600777]

47. Nieto L, Moratal D, Marti-Bonmati L, Alberich A, Galant J. [Morphological characterization of trabecular bone structure using high resolution magnetic resonance imaging]. Radiologia. 2008; 50(5):401–408. [PubMed: 19055918]

48. Nakagawa S, Kadoya Y, Todo S, Kobayashi A, Sakamoto H, Freeman MA, et al. Tibiofemoral movement 3: full flexion in the living knee studied by MRI. The Journal of bone and joint surgery British volume. 2000; 82(8):1199–1200. [PubMed: 11132287]

49. Muriuki MG, Tuason DA, Tucker BG, Harner CD. Changes in tibiofemoral contact mechanics following radial split and vertical tears of the medial meniscus an in vitro investigation of the efficacy of arthroscopic repair. The Journal of bone and joint surgery American volume. 2011; 93(12):1089–1095. [PubMed: 21571989]

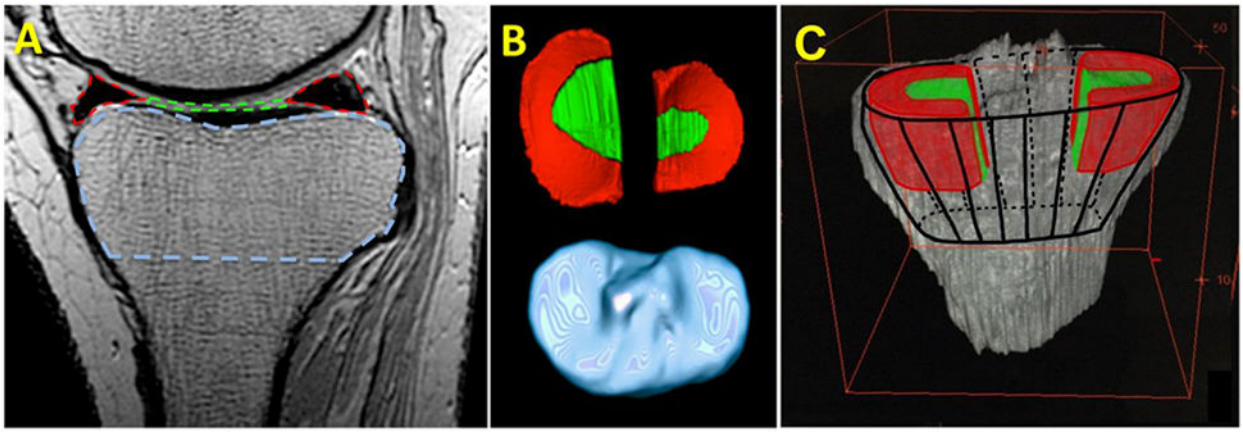

Figure 1.

(**A**) high-resolution 3D CUBE sagittal MR image of a cadaveric knee overlaid with the outlines segmenting the menisci (red), meniscus-uncovered region (green), and trabecular bone and marrow of the proximal tibia (blue). 3D visualization of (**B**) the segmented menisci (red), meniscus-uncovered regions (green), and the proximal tibia (blue), (**C**) projected axially onto the trabecular regions of the proximal tibia to create four volumes of interest.

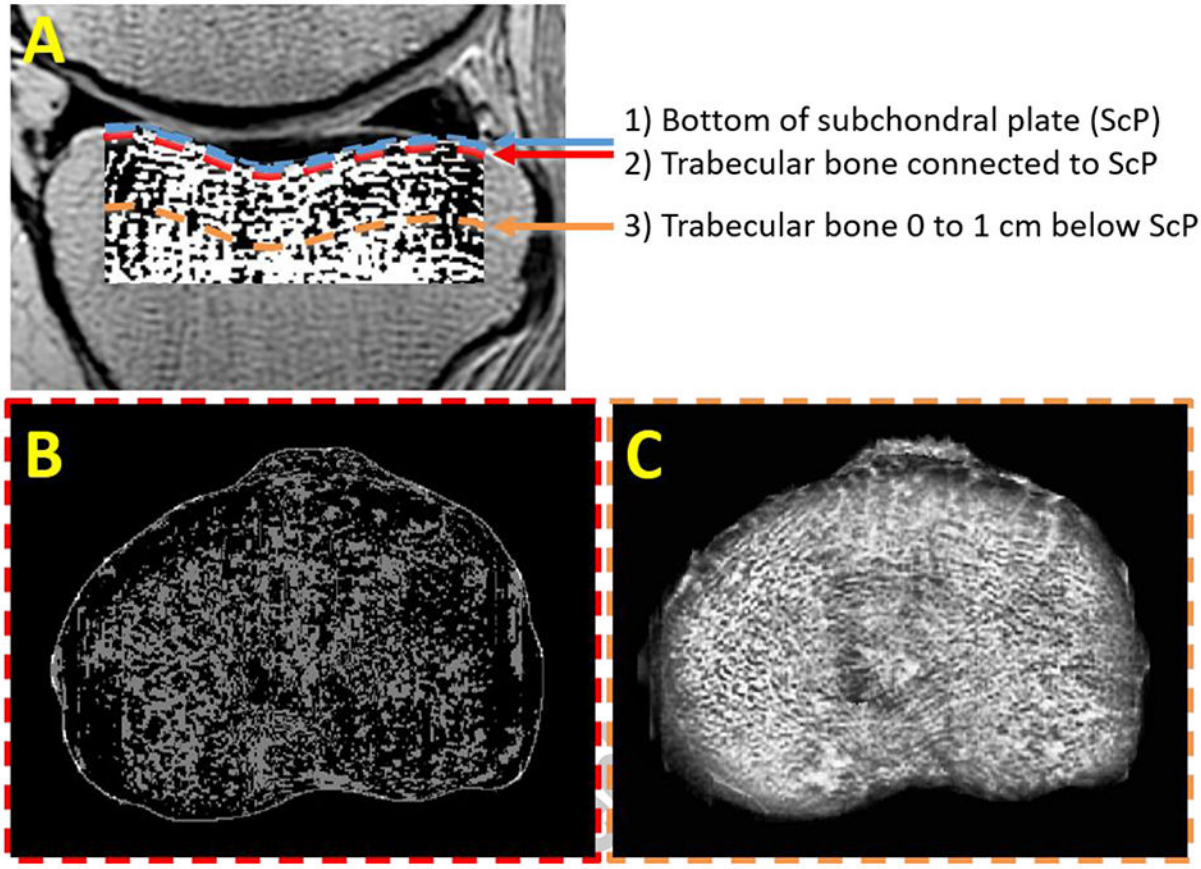

Figure 2.

Schematic of proximal tibia (**A**) showing the bottom of the subchondral plate (ScP) (top blue line), a layer 0.25 mm below the ScP (middle red line) and a slab 10 mm below ScP (bottom orange line). Axially-flattened mean intensity projection image of 0.25-mm-thick ScP connected bone (**B**) and 10-mm thick slab of trabecular bone (**C**).

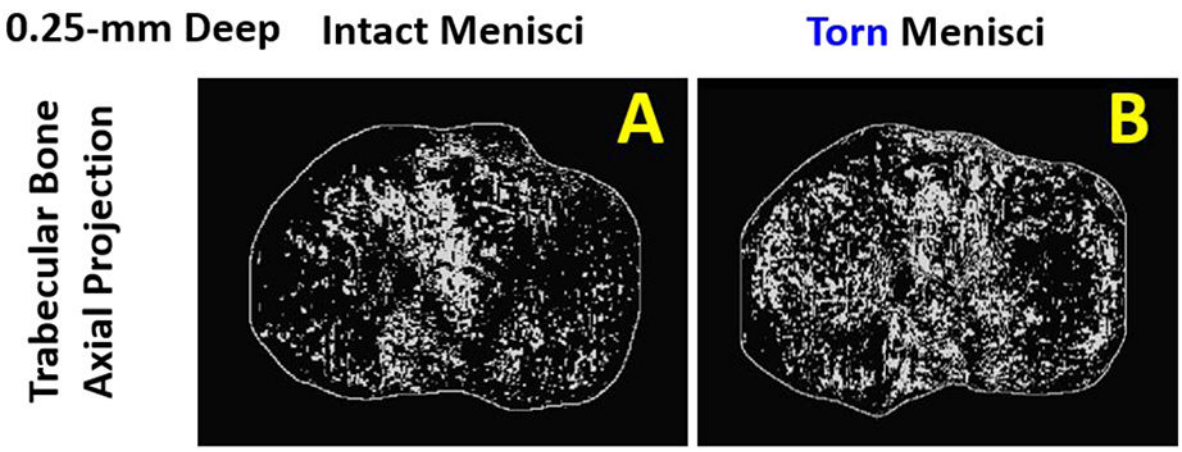

Figure 3.

Axial mean intensity projection images of the subchondral plate connected trabeculae in a knee with intact menisci (**A**) and another knee with torn medial and lateral menisci (**B**).

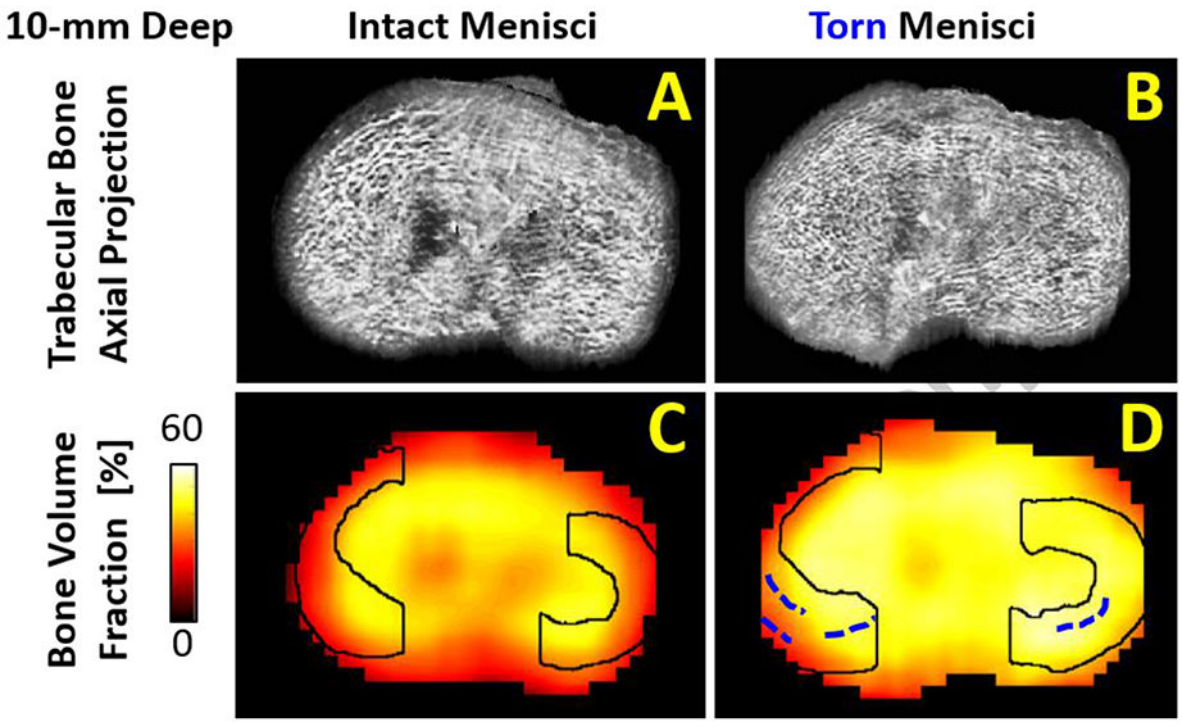

Figure 4.

Axial mean intensity projection images of trabeculae of the 10-mm thickness slab beneath the ScP in a knee with intact menisci (**A**) and another knee with torn bilateral menisci (**B**). Color maps of apparent bone volume fraction in the knee with intact menisci (**C**) and torn menisci (**D**) suggested variations with meniscus coverage as well as integrity. Meniscal tear (blue dotted lines, **D**) at posterior horns.

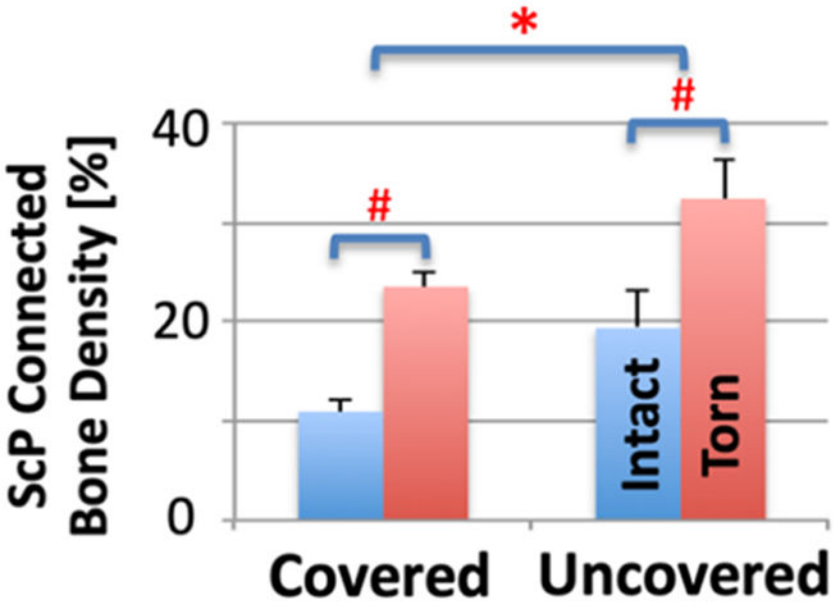

Figure 5.

Mean values with a standard error of the mean (error bars) of apparent ScP connected bone density separated by location (meniscus-covered vs. -uncovered regions) and meniscal integrity (intact vs. torn). * = significant ($p<0.05$) difference between meniscus-covered and -uncovered region. # = significance different between intact menisci and torn menisci.

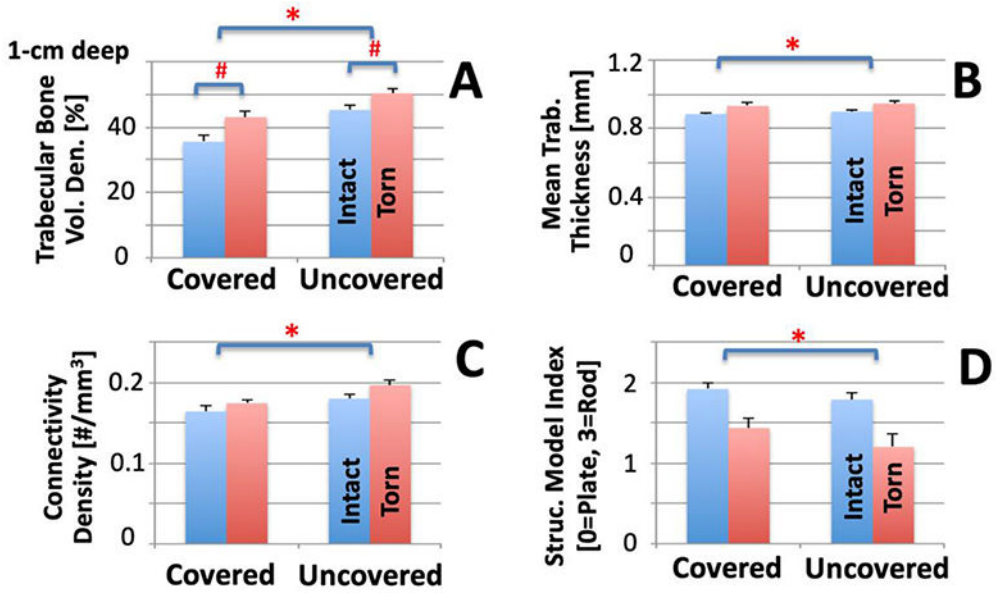

Figure 6.

Mean value with a standard error of the mean (error bars) of apparent bone volume fraction (**A**), apparent mean trabecular thickness (**B**), apparent connectivity density (**C**), and structure model index (**D**) separated by location (meniscus-covered vs. -uncovered regions) and meniscal integrity (intact vs. torn). There was significant higher value of all parameters of meniscus-uncovered region compared to meniscus-covered region in both groups (intact and torn menisci). * = significant ($p<0.05$) difference between meniscus-covered and -uncovered region. # = significance different between intact menisci and torn menisci.

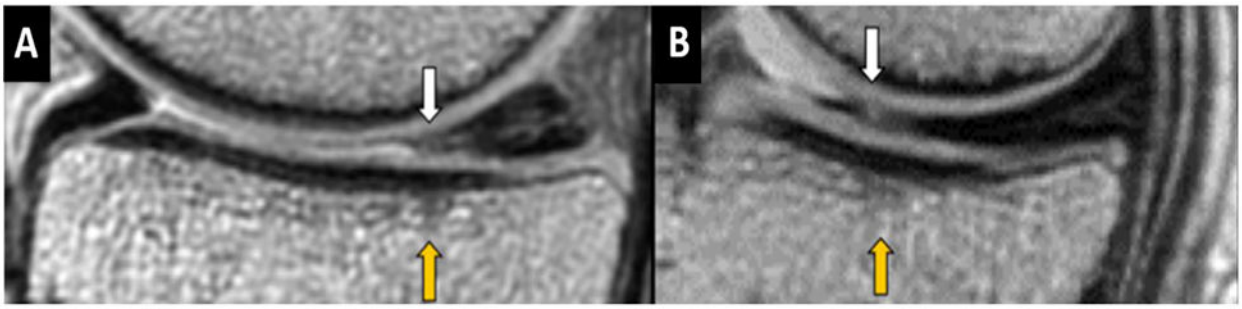

Figure 7.

Sagittal plane (**A**) and coronal plane (**B**) of high-resolution MR image (3D CUBE) showed small radial tear at posterior horn of lateral meniscus (white arrows) and focal increased trabeculae in lateral tibial plateau beneath the small tear (orange arrows).

Table 1.

Meniscal pathology in six cadaveric knees

Knee No.	Donor No.	Medial meniscus	Lateral meniscus
1	1	Intact	Intact
2	1	Intact	Tear at the body
3	2	Tear at the posterior horn	Tear at the body
4	2	Tear at the body and the posterior horn	Tear at the anterior horn and the body
5	3	Tear at the body and the posterior horn	Tear at the posterior horn
6	3	Tear at the body and the posterior horn	Tear at the body and the posterior horn

Table 2.

The mean values (standard error of the mean) of MR bone measures across location and meniscal integrity as well as p-value from two-way ANOVA.

MR bone measures	Mean (standard error)				P-values (post hoc power)		
	Intact menisci		Torn menisci				
	Covered	Uncovered	Covered	Uncovered	Intact vs. Torn	Cover vs. uncover	Interaction ≠
ScP connected bone density, %	10.9 (1.2)	19.3 (3.9)	23.5 (1.4)	32.4 (3.9)	0.007 * (0.34)	0.048 * (0.49)	0.956 (0.95)
App BVF (%)	35.5 (1.8)	45.2 (1.3)	43.0 (1.9)	50.3 (1.3)	0.047 * (0.24)	<0.001 * (0.12)	0.360 (0.36)
App Tb.Th (mm)	0.88 (0.010)	0.90 (0.008)	0.93 (0.018)	0.95 (0.015)	0.136 (0.98)	0.030 * (0.05)	0.993 (0.99)
App CD (#/cm^3)	0.16 (0.007)	0.18 (0.005)	0.17 (0.005)	0.20 (0.006)	0.176 (0.46)	0.002 * (0.63)	0.485 (0.49)
SMI (0=Plate, 3=Rod)	1.92 (0.08)	1.79 (0.09)	1.43 (0.13)	1.20 (0.16)	0.059 (0.91)	0.015 * (0.04)	0.419 (0.42)

Note Cover = Trabeculae beneath meniscus-covered region, Uncover = Trabeculae beneath meniscus-uncovered region, ScP = Subchondral plate, App BVF = Apparent bone volume fraction, App Tb.Th = Apparent trabecular thickness, App CD = Apparent connectivity density, SMI = Structure model index

* = Significant p-value less than 0.05

≠ = Interaction between meniscal integrity and meniscal coverage